A Comparison among High Power Factor Integrated Electronic Ballasts with Similar Ideas

Tiago B. Marchesan, Alysson R.Seidel, Fábio E. Bisogno and Ricardo N. do Prado

Researching Group of Electronic Ballasts - GEDRE
PPGEE - NUPEDEE – CT
Federal University of Santa Maria
97105-900 - Santa Maria - RS – Brazil
rnprado@ieee.org

***Abstract* - This paper provides a comparative analysis among four electronic ballasts topologies with high power factor, employing the same switch for inverter and power factor correction stage based on experimental results. An electromagnetic Ballast analysis is included to provide a comparison with implemented electronic ballasts. Then, it is shown features of each topology through their advantages and disadvantages. The electronic ballasts topologies are done for two 40 W fluorescent lamps at 50 kHz switching frequency and 110 V RMS, 60 Hz utility line.**

I. INTRODUCTION

A great amount of the electric energy produced in the world is consumed as artificial illumination, and any improvement in the efficiency of illuminating systems is desirable [1]. These systems when using fluorescent lamps reduce the consumption of electric energy when compared to incandescent lamps, because the former presents higher efficacy (lm/W) [2].

In recent years several topologies were developed improving the performance of fluorescent lamps when it is supplied for electronic systems instead of electromagnetic systems, such as a Boost Half-Bridge Integrated converter (EBBH) [3], Flyback Half-Bridge Integrated Converter (EBFH) [4], Boost Push-Pull Integrated Converter (EBBP) [5], Flyback Push-Pull Integrated Converter (EBFP) [6]. The topologies with a single stage power factor correction became more attractive in industry, due to they have light weight, lower flicker level, high power factor, and high efficiency, if compared with conventional ballasts [3].

Unity power factor is given by the Boost or Flyback converter operating in discontinuous conduction mode. The lamp high frequency supply is given by the Half-Bridge or Push-Pull converter. The lamp is supplied by a series-parallel resonant filter LCC that provides sinusoidal voltage and current waveforms into the lamp, guaranteeing low crest factor and longer useful life. An electromagnetic interference filter EMI, provides a low harmonic distortion and consequently a high power factor for the utility line.

This paper is organized as follows. In section II the electronic topologies are shown, in section III the design procedure and operational principles of electronic ballasts are cited. In section IV experimental results for electronic and electromagnetic topologies are presented, and in section V a comparative analysis is demonstrated among the topologies presented based on experimental results.

II. ELECTRONIC BALLASTS TOPOLOGIES

The topologies configurations are shown in Fig. 1. Fig.1(a) shows the electronic ballast employing Boost Half-Bridge integrated converter (EBBH), and Fig. 1(b), (c), and (d) show the electronic Ballast with Flyback Half-Bridge integrated converter (EBBH), electronic ballast with Boost Push-Pull integrated converter (EBBP), and electronic ballast Flyback Push-Pull integrated converter (EBFP) respectively.

All topologies are formed by a single-phase voltage supply V_{in}, an input rectifier, an Electromagnetic Interference filter, a power factor circuit, a power switch (1 or 2), an inverter stage, a series-parallel resonant filter, LCC, and two 40 W fluorescent lamps.

III. ELECTRONIC BALLASTS DESIGN PROCEDURE

The topologies are designed for two 40 W fluorescent lamps, for input line 110 VRMS, 60 Hz, and switching frequency of 50 kHz. The behavior of each topology along with their operation principle and relevant equations are described in details.

A. Series-Parallel Resonant Filter

The LCC series parallel resonant filter is one of the simplest and more commonly used resonant circuits suitable for driving fluorescent lamps. The filter components are calculated by (1) and (2), through the θ phase angle in Fig. 2.

$$C_p = \sqrt{\frac{[1+(\tan(\theta))^2]\,.\,P}{\omega^2.R.V_{ac}^{\,2}} - \frac{1}{\omega^2.R^2}} \qquad (1)$$

$$L(\theta, Cs) = \frac{R.\tan(\theta) + C_p(\theta).R^2.\omega}{\omega.\left[1+\omega^2.\left(C_p(\theta)\right)^2.R^2\right]} + \frac{1}{C_s.\omega^2} \qquad (2)$$

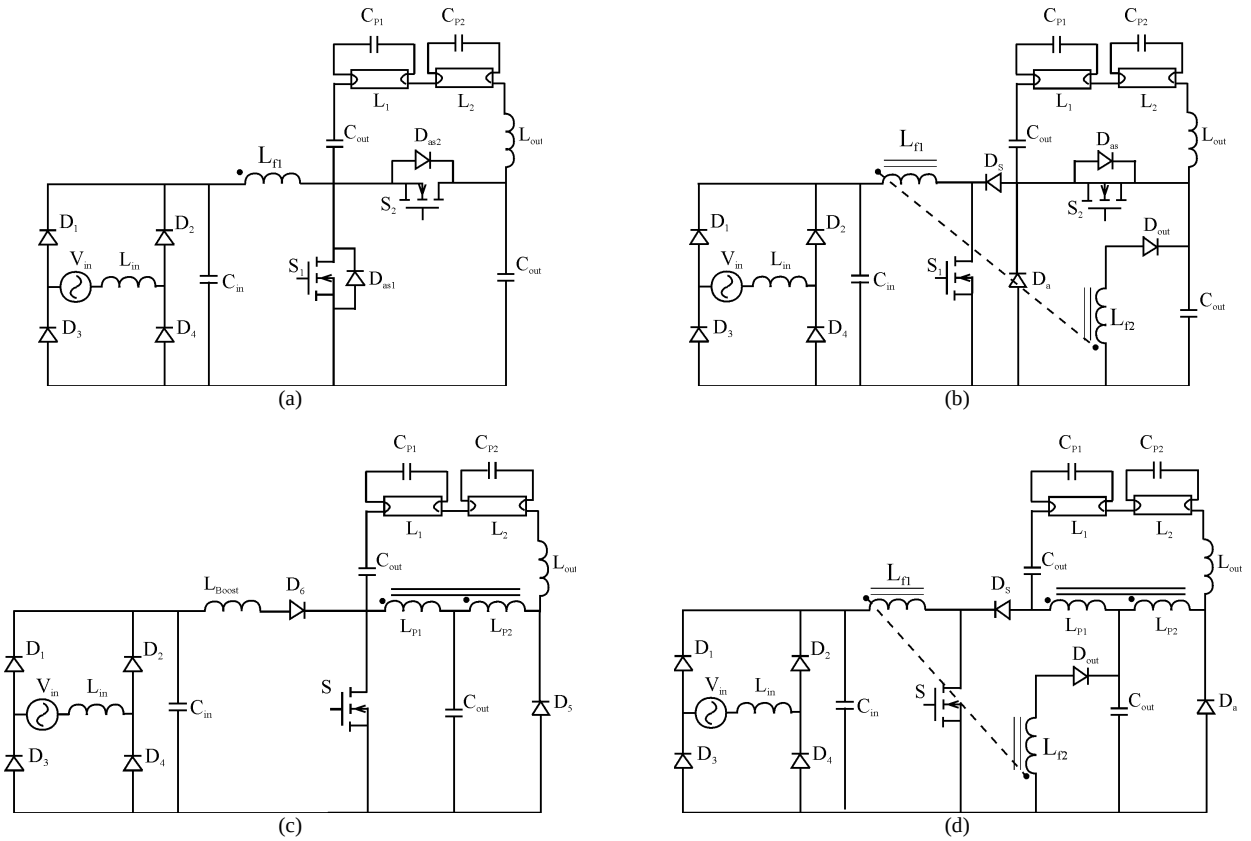

Fig.1. Electronic Ballasts Topologies: (a) EBBH, (b) EBFH, (c) EBBP, (d) EBFP

Where:

$C_P(\theta)$	parallel capacitor resonant
θ	impedance phase angle
P	lamp power
ω	angular switching frequency
f_s	switching frequency
R	lamp equivalent resistance
V_{ac}	rms voltage of the fundamental component
C_s	series capacitor resonant

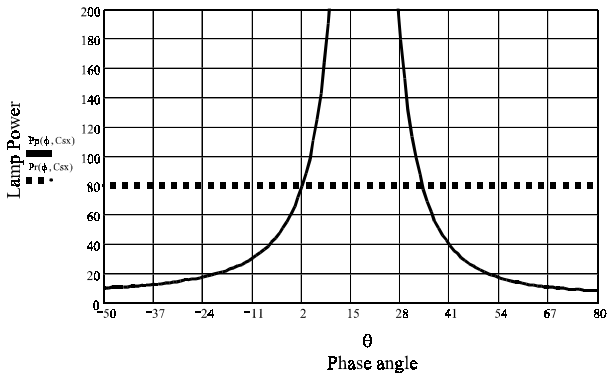

Fig. 2. Power in the Lamp

B. Boost Inductance

The L_{boost} inductor is obtained from the following equation:

$$\alpha = \frac{V_{max}}{V_0} \tag{3}$$

$$D = 1 - \alpha \tag{4}$$

$$Y_1(\alpha) = -2 - \frac{\pi}{\alpha} + \frac{2}{\alpha\sqrt{1-\alpha^2}} \cdot \left[\frac{\pi}{2} + \tan^{-1}\left(\frac{\alpha}{\sqrt{1-\alpha^2}}\right)\right] \tag{5}$$

$$L_{boost} = \frac{V^2_{max}}{\omega . P_{out}} \cdot \frac{(1-\alpha)^2 . Y_1(\alpha)}{\alpha} \tag{6}$$

C. Flyback Inductance

To guarantee discontinuous conduction mode, the inductances of the flyback windings must be consider.

The flyback inductor (L_{f1}) current is shown in (7),

$$I_{Lf1max} = I_{in,peak} = \frac{V_{in} . D_{max}}{L_{f1.} f_s} \tag{7}$$

and the current in the secondary windings of the flyback (L_{f2}) is determined by (8).

$$I_{Lf2max} = I_{Lf1max} + \frac{V_{cout} . t_{off}}{L_{f1} . f_s} = I_{Lf1max} + \frac{V_{cout(1-D_{max})}}{L_{f2} . f_s} \tag{8}$$

Where:

L_{f1}	flyback primary winding
L_{f2}	flyback secondary winding
$I_{Lf1\ max}$	maxim current in the flyback primary winding
$I_{in,\ peak1}$	input peak current
$I_{Lf2\ max}$	maxim current in the flyback secondary winding
$I_{in,\ peak2}$	input peak current
D_{max}	maxim duty cycle
D	duty cycle
t_{off}	demagnetizing time
V_{cout}	output voltage

VI. EXPERIMENTAL RESULTS

In order to verify the proposed comparison between four electronic ballasts these prototypes have been implemented to meet the input data specifications according to Fig.1. An electromagnetic ballast was analyzed to make a comparison with the other four electronic topologies that was implemented. The main parameters are as follows:

An electromagnetic ballast

- PRELETRI electromagnetic ballast
- Supply Voltage: V_{in} = 220 V RMS, 60Hz;
- Output Power: P_o = 2 x 40W;
- Power Factor higher than 0,93

Four electronic ballasts

- Supply Voltage: V_{in} = 110 V RMS, 60Hz;
- Output Power: P_o = 80W;
- Switching frequency: f_s = 50kHz

A high frequency input filter, L_{in} and C_{in}, which reduces switching harmonic current, was used with the following parameters:

- L_{in}: 1.4 mH, 160 turns on core EE 20/10 IP6-Thornton;
- C_{in}: 680 nF/250 V (polypropylene);

The parameters and components of the complete power diagrams for the following electronic topologies are:

A. Electronic Ballast Boost Half-Bridge Integrated Converter

The circuit parameters are:

- R_{Lamp1}, R_{Lamp2}: F40D (Osram);
- Diode rectifier bridge D_1-D_4: 1N4004.
- L_{Boost}: 490 µH, 160 turns, EE 20/10 IP6-Thornton;
- D_B: Boost diode: UF4007;
- S_1, S_2: IRF 740 (International Rectifiers);
- C_{out}: 220 µF/ 350 V (electrolytic);

A high frequency series-parallel resonant filter LCC, L_{out}, C_P, C_S, which eliminates the highest output current order harmonic components is employed. Its parameters are as follows:

- L_{out}: 1.22 mH 160 turns, EE 20/10 IP6-Thornton;
- C_S: 150 nF/250 V (polypropylene);
- C_P: 8.2 nF/250 V (polypropylene);

B. Electronic Ballast Flyback Half-Bridge Integrated Converter

The circuit parameters are:

- R_{Lamp1}, R_{Lamp2}: F40D (Osram);
- Diode rectifier bridge D_1-D_4: 1N4004;
- L_{f1}: 295 µH, 48 turns, EE 20/10 IP6-Thornton;
- L_{f2}: 497 µH, 60 turns, EE 20/10 IP6-Thornton;
- D_a, D_S, D_{out}: UF4007;
- S_1, S_2: IRF 740 (International Rectifiers);

A high frequency series-parallel resonant filter LCC, L_{out}, C_P, C_S, which eliminates the highest output current order harmonic components is employed. Its parameters are as follows:

- L_{out}: 1 mH, 150 turns, EE 20/10 IP6-Thornton;
- C_S: 150 nF/250 V (polypropylene);
- C_P: 10 nF/250 V (polypropylene);

C. Electronic Ballast Boost Push-Pull Integrated Converter

The circuit parameters are:

- R_{Lamp1}, R_{Lamp2}: F40D (Osram);
- Diode rectifier bridge D_1-D_4: 1N4004.
- L_{Boost}: 253 µH, 150 turns, EE 20/10 IP6-Thornton;
- L_{P1}, L_{P2}: 1.6 mH, 120 turns, EE 20/10 IP6-Thornton;
- D_a, D_S, D_{out}: UF4007;
- S_1: IRF 740 (International Rectifiers);

A high frequency series-parallel resonant filter LCC, L_{out}, C_P, C_S, which eliminates the highest output current order harmonic components is employed. Its parameters are as follows:

- L_{out}: 1.8 mH, 150 turns, EE20/10 IP6-Thornton;
- C_S: 22 nF/400V(polypropylene);
- C_{P1}, C_{P2}: 8.2 nF/600V(polypropylene);

D. Electronic Ballast Flyback Push-Pull Integrated Converter

The circuit parameters are

- R_{Lamp1}, R_{Lamp2}: F40D (Osram);
- Diode rectifier bridge D_1-D_4: 1N4004.
- L_{f1}: 1.2 mH, 48 turns, EE 20/10 IP6-Thornton;
- L_{f2}: 1.45 mH, 60 turns, EE 20/10 IP6-Thornton;

- L_{P1}, L_{P2}: 1.6 mH, 120 turns, EE 30/14 IP6-Thornton;
- D_a ,D_S: UF4007;
- S_1: IRF 740 (International Rectifiers);

A high frequency series-parallel resonant filter LCC, L_{out}, C_P, C_S, which eliminates the highest output current order harmonic components is employed. Its parameters are as follows:

- L_{out}: 1.7 mH, 160 turns, EE 20/10 IP6-Thornton;
- C_S: 22 nF/250 V (polypropylene);
- C_{P1}, C_{P2}: 8.2 nF/250 V (polypropylene);

Fig.3 shows experimental waveforms for EBBH. Fig.3(a) shows the line current and voltage. These illustrations show the high-power-factor of this electronic ballast topology. Fig.3(b) shows the current of the boost inductor in high frequency in discontinuous conduction mode. Fig.3(c) shows the switch voltage and current. Fig.3(d) shows the lamp and current voltage in high frequency with quasi sinusoidal waveform and low crest factor current.

Fig.4 shows the waveforms for EBFH. Fig.4(a) shows the line current and voltage. These illustrations showing the high-power-factor of this electronic ballast topology. Fig.4(b) shows the flyback inductor current in high frequency in discontinuous conduction mode. Fig.4(c) shows the switch voltage and current. Fig.4(d) shows the lamp and current voltage in high frequency with quasi sinusoidal waveform and low crest factor current.

Fig.5 shows the waveforms for EBBP. Fig.5(a) shows line current and voltage. These illustrations show the high-power-factor of this electronic ballast. Fig.5(b) shows the current of the boost inductor in high frequency in discontinuous conduction mode. Fig.5(c) shows the switch voltage and current. Fig.5(d) shows the lamp and current voltage in high frequency with quasi sinusoidal waveform and low crest factor.

Fig.6 shows the waveforms for EBFP. Fig.6(a) shows the line current and voltage. These illustrations show the high-power-factor of this electronic ballast. Fig.6(b) shows the current of the Flyback inductor in high frequency in discontinuous conduction mode. Fig.6(c) shows the switch voltage and current. Fig.6(d) shows the lamp and current voltage in high frequency.

Fig.7 shows the waveform for the electromagnetic ballast. Fig. 7(a) shows the line current and voltage and Fig. 7 (b) shows the lamp current and voltage.

Experimental data were obtained through the scope tektronix TDS430A and analyzed by the software MathCad.

VI. COMPARISONS AMONG THE DESCRIBED BALLASTS

In this paper, the comparison aspects can be characterized as follows: steady state performance, abnormal operation, suitability for multi-lamp connection, starting voltage and other characteristics shown in Table I.

The use of Flyback converter or Boost converter to obtain a high-power-factor provided near unity power-factor correction for both converters with the same features for this power range.

Table I shows the performance of each converter.

In the inverter stage, it is employed a Half-Bridge inverter or a Push-Pull inverter. The topologies that employ the Half-Bridge inverter present advantages such as ZVS and higher efficiency.

The Push-Pull inverter presents advantages such as the use of a single switch that simplifies the drive circuit, decreasing costs, and increasing the reliability of the topology.

An electromagnetic ballast (EMB) was analyzed to make a comparison with the other four electronic ballasts that was implemented.

TABLE I
Comparisons Among the Ballasts Studied

	EBBH	**EBFH**	**EBBP**	**EBFP**	**EMB**
Switches	2	2	1	1	-
Inductor	3	3	4	4	-
Switch Voltage Stress	$0,75.V_{ns}$	$1.V_{ns}$	$1.V_{ns}$	$0,75.V_{ns}$	-
Switch Current Stress	$0,4.I_{ns}$	$0,5.I_{ns}$	$0,25.I_{ns}$	$0,6.I_{ns}$	-
Current crest Factor	1,24	1,35	1,54	1,47	1,54
Total Harmonic Distortion	0,023	0,033	0,154	0,044	0,222
Power Factor	0,990	0,987	0,991	0,997	0,96
Audible Noise Absence	Yes	Yes	Yes	Yes	No
Flicker Absence	Yes	Yes	Yes	Yes	No
Efficacy (%)	92,7	91,0	86,0	89,4	80,1

VII. CONCLUSION

This paper introduces a comparison among four topologies, and analyzes the performance of each one giving physical insight of electronic ballasts and provides background knowledge for designers to selecting an appropriate one. The theoretical discussion and analysis were verified through experimental results. According to these results it was verified that each topology presents a specific application, so EBBH presents higher efficacy, high performance, low switches stress with ZVS, for both switches.

The EBFH presents the same characteristics, but is better when compared its employment in input line ac of 220 V RMS ac.

As the topologies which employ Push-Pull converter presents: fewer components and less efficacy than the Half-Bridge converter. Push-Pull is suggested for occasions when their higher power is necessary.

The topologies which use Flyback Converter for power factor correction have the advantage of operating with an input line ac of 220 V RMS

The main advantage of the topologies presented was the use of integrated stages power conversion with the same switch achieving a near unity power factor, reduced current harmonic distortion, and consequently a better use of the input line.

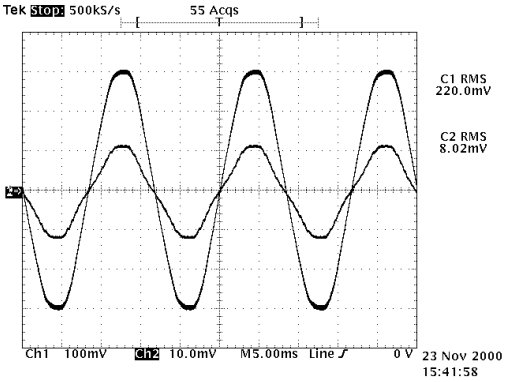

(a)

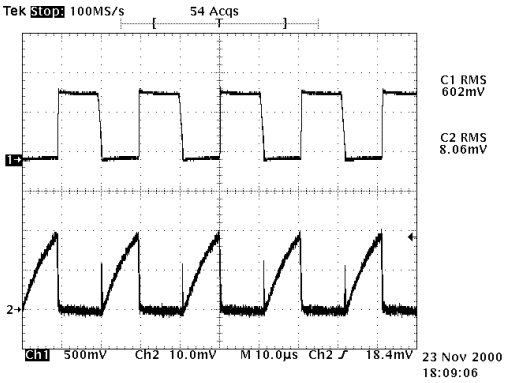

(b)

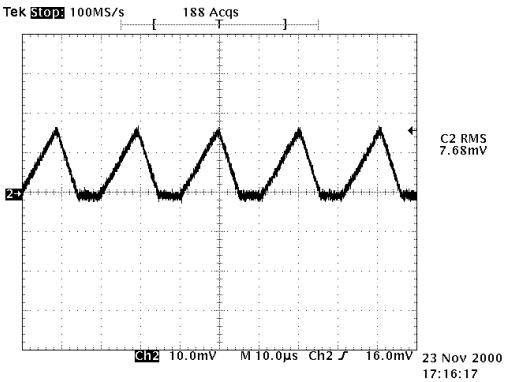

(c)

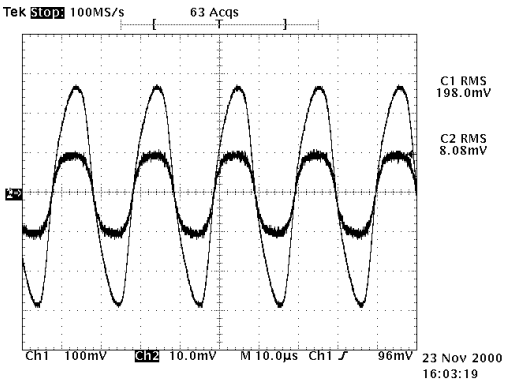

(d)

Fig. 3. EBBH waveforms (a) Input Voltage and Current(50 V/div; 1A/div;5ms); (b)Power Switch Voltage and Current;(250 V/div; 2A/div;10µs) (c) Boost Inductor current;(2A/div;10µs) (d) Voltage and current in the lamp(50 V/div;500mA/div;10µs).

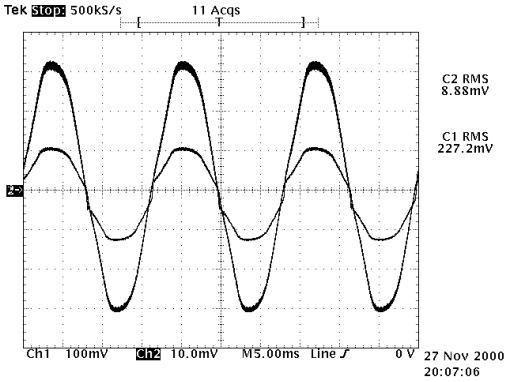

(a)

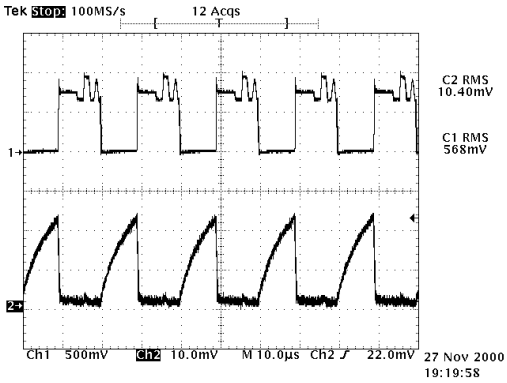

(b)

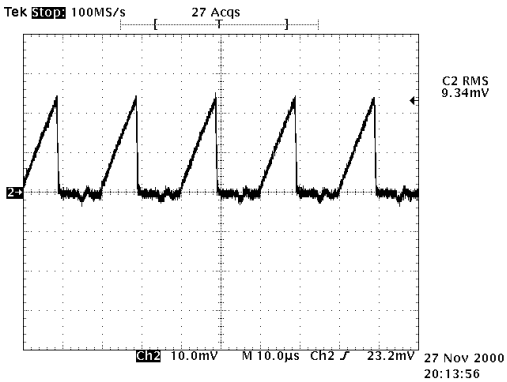

(c)

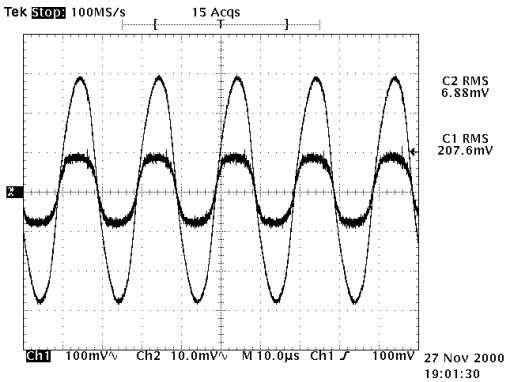

(d)

Fig. 4. EBFH waveforms (a) Input Voltage and Current(50 V/div; 2A/div;5ms); (b)Power Switch Voltage and Current;(250 V/div; 2A/div;10µs) (c) Boost Inductor current;(2A/div;10µs) (d) Voltage and current in the lamp(50 V/div;500mA/div;10µs).

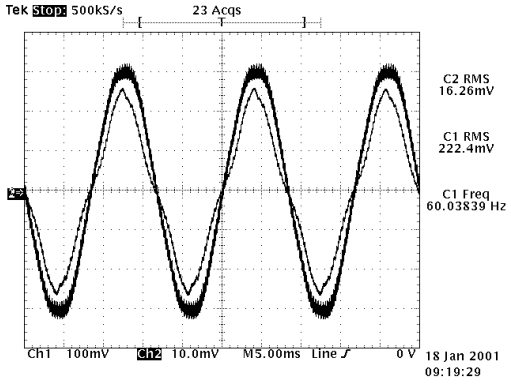

(a)

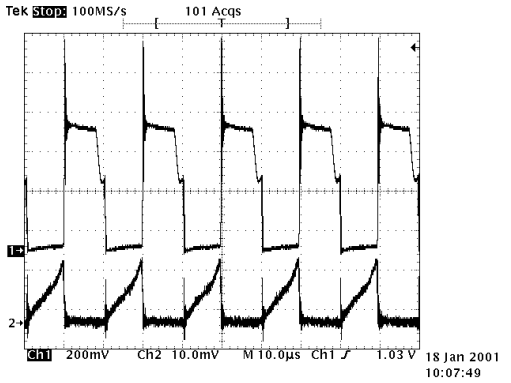

(b)

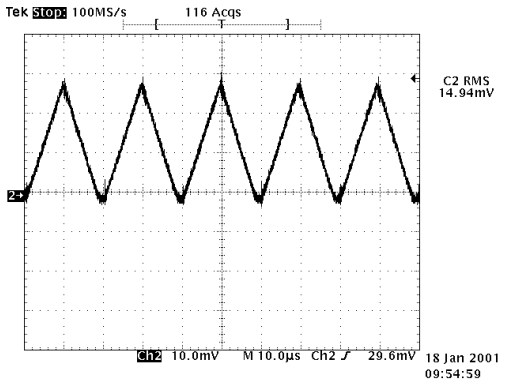

(c)

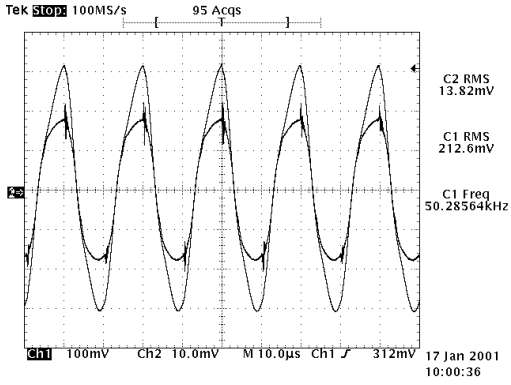

(d)

Fig. 5. EBBP waveforms, (a) Input Voltage and Current (50V/div; 500mA/div; 5ms); (b) Power Switch Voltage and Current (100V/div; 5A/div; 10µs); (c) Boost Inductor Current (1A /div; 10µs); (d) Voltage and Current in the Lamp (50V/div; 500mA/div; 10µs).

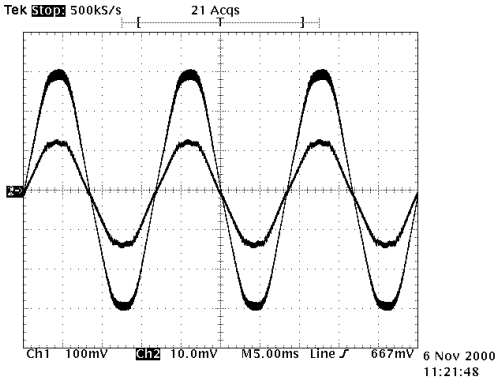

(a)

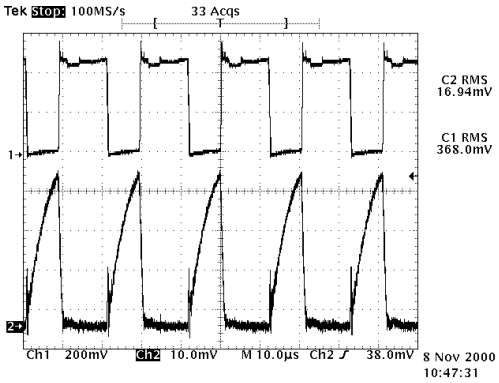

(b)

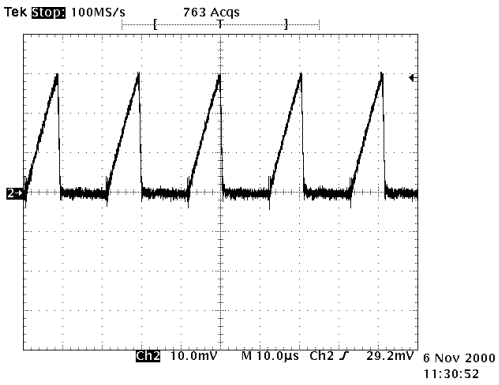

(c)

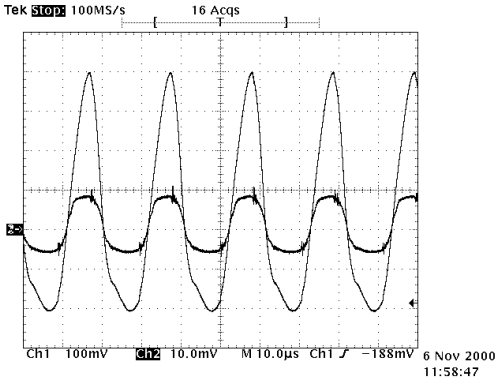

(d)

Fig. 6. EBFP waveforms, (a) Input Voltage and Current (50V/div; 1A/div; 5ms); (b) Power Switch Voltage and Current (100V/div; 2A/div; 10µs); (c) Flyback Inductor Current (2A/div; 10µs); (d) Voltage and Current in the Lamp (50V/div; 500mA/div; 10µs).

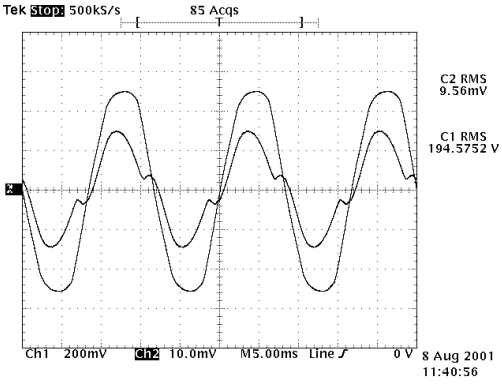

(a)

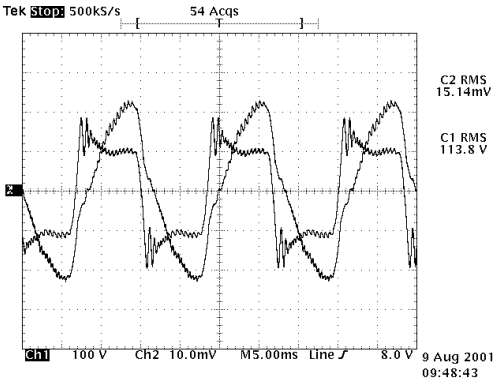

(b)

Fig. 7. EMB waveforms (a) Input Voltage and Current (100V/div; 500mA/div; 5ms) ; (b) Voltage and Current in the Lamp (100V/div; 500mA; 5ms).

This topology operating in high frequency allows consuming an average of 20-25 percent less energy from the same light output. The electronic ballasts topologies present low weight, flicker absence, and audible noise absence. Experimental results have been obtained for two 40W fluorescent lamps operating at 50kHz, and 110V line voltage, 60Hz and all electronic ballasts topologies presented higher efficacy than 86%.

REFERENCES

[1] T. H. Yu and L. M. Wu. "Comparisons among Self-Excited Parallel Resonant, Series Resonant and Current-Fed Push-Pull Electronic Ballasts", IEEE Applied Power Electronic Conference, pp. 421-426, 1994.

[2] J. M. Alonso, A. L Colleja, E. Lópes, J. Ribas, FJ. Ferrero and M. Rico. Analysis and Experimental Results of a single Stage High-Power-Factor Electronic Ballast Based on Flyback Converter. IEEE Applied Power Electronic Conference, 1998, record.

[3] R. N. Prado, S. A, M. F. Silva, M. Jungbeck, A. R. Seidel "Low Cost High Power Factor Electronic Systems for Compact Fluorescent Lamps", IEEE IAS'99, record.

[4] R. N. do Prado, S. A. Bonaldo "Designing a Dimmable High Power Electronic Ballast for Fluorescent Lamps", IEEE PESC'99, record.

[5] R. N. do Prado, and S. A. Bonaldo, "A High-Power-Factor Electronic Ballast using a Flyback Push-Pull Integrated Converter", IEEE Trans. Industrial Electron, vol. 46, pp 796-802.

[6] R. N. do Prado, A. R. Seidel, F. E. Bisogno. T. B. Marchezan. "A Boost Push-Pull Electronic Ballast with a Single Switch"IECON 2000, record.

[7] R. N. do Prado, A. R. Seidel, F. E. Bisogno. M. A. D. Costa, "Self-Oscillating electronic Ballast Design" IECON 2000, record.